

**Pulses of enhanced
North Pacific
Intermediate Water
ventilation**

L. Max et al.

**Pulses of enhanced North Pacific
Intermediate Water ventilation from the
Okhotsk Sea and Bering Sea during the
last deglaciation**

L. Max¹, L. Lembke-Jene¹, J.-R. Riethdorf², R. Tiedemann¹, D. Nürnberg²,
H. Kühn¹, and A. Mackensen¹

¹Alfred-Wegener-Institut, Helmholtz-Zentrum für Polar- und Meeresforschung,
Am Handelshafen 12, 27570 Bremerhaven, Germany

²GEOMAR, Helmholtz-Zentrum für Ozeanforschung Kiel, Wischhofstr. 1–3,
24148 Kiel, Germany

Received: 11 October 2013 – Accepted: 27 October 2013 – Published: 7 November 2013

Correspondence to: L. Max (lars.max@awi.de)

Published by Copernicus Publications on behalf of the European Geosciences Union.

Title Page

Abstract

Introduction

Conclusions

References

Tables

Figures

⏪

⏩

◀

▶

Back

Close

Full Screen / Esc

Printer-friendly Version

Interactive Discussion

Abstract

Under modern conditions only North Pacific Intermediate Water is formed in the Northwest Pacific Ocean. This situation might have changed in the past. Recent studies with General Circulation Models indicate a switch to deep-water formation in the Northwest Pacific during Heinrich Stadial 1 (17.5–15.0 kyr) of the last glacial termination. Reconstructions of past ventilation changes based on paleoceanographic proxy records are still insufficient to test whether a deglacial mode of deep-water formation in the North Pacific Ocean existed. Here we present deglacial ventilation records based on radiocarbon-derived ventilation ages in combination with epibenthic stable carbon isotopes from the Northwest Pacific including the Okhotsk Sea and Bering Sea, the two potential source regions for past North Pacific ventilation changes. Evidence for most rigorous ventilation of the mid-depth North Pacific occurred during Heinrich Stadial 1 and the Younger Dryas, simultaneous to significant reductions in Atlantic Meridional Overturning Circulation. Concurrent changes in $\delta^{13}\text{C}$ and ventilation ages point to the Okhotsk Sea as driver of millennial-scale changes in North Pacific Intermediate Water ventilation during the last deglaciation. Our records additionally indicate that changes in the $\delta^{13}\text{C}$ intermediate water (700–1750 m water depth) signature and radiocarbon-derived ventilation ages are in antiphase to those of the deep North Pacific Ocean (>2100 m water depth) during the last glacial termination. Thus, intermediate and deep-water masses of the Northwest Pacific have a differing ventilation history during the last deglaciation.

1 Introduction

Today, the renewal of North Pacific Intermediate Water (NPIW) is mainly coupled to physical processes in the Okhotsk Sea (Talley and Roemmich, 1991; Talley, 1993), where Dense Shelf Water is produced in coastal polynyas by brine rejection during wintertime sea-ice production (Shcherbina et al., 2003). These water masses leave

CPD

9, 6221–6253, 2013

Pulses of enhanced North Pacific Intermediate Water ventilation

L. Max et al.

Title Page

Abstract

Introduction

Conclusions

References

Tables

Figures

⏪

⏩

◀

▶

Back

Close

Full Screen / Esc

Printer-friendly Version

Interactive Discussion

Pulses of enhanced North Pacific Intermediate Water ventilation

L. Max et al.

[Title Page](#)

[Abstract](#)

[Introduction](#)

[Conclusions](#)

[References](#)

[Tables](#)

[Figures](#)

[⏪](#)

[⏩](#)

[◀](#)

[▶](#)

[Back](#)

[Close](#)

[Full Screen / Esc](#)

[Printer-friendly Version](#)

[Interactive Discussion](#)

the Okhotsk Sea as Okhotsk Sea Intermediate Water (OSIW), mix with water in the Northwest Pacific at intermediate depths and form NPIW (Yasuda, 1997). The NPIW spreads eastward through the North Pacific Ocean between ca. 20° N–40° N. Its easternmost extension is located in the vicinity of the California Current region, where it can still be recognized as a well-defined water mass of higher oxygen concentrations between ca. 300–800 m water depth (Talley, 1993). The deep North Pacific (> 2000 m water depth) (Talley et al., 2003) is only slowly replenished by Southern Ocean water masses due to the absence of deep-water formation in the North Pacific Ocean today (Warren, 1983; Emile-Geay et al., 2003).

Several studies with General Circulation Models (GCMs) point to fundamental changes in deep Pacific hydrography and circulation during the last deglaciation (Mikolajewicz et al., 1997; Schmittner et al., 2007; Okumura et al., 2009; Okazaki et al., 2010; Chikamoto et al., 2012; Menviel et al., 2012). A few model simulations show an onset of deep-water formation to a depth of ~ 2500 to 3000 m in the Northwest Pacific during deglacial cold events Heinrich Stadial 1 (HS-1) and the Younger Dryas (YD) due to a breakdown of the salinity driven stratification (Okazaki et al., 2010; Menviel et al., 2012). In these scenarios, a larger northward advection of heat and salt into the subarctic Pacific known as Stommel feedback (Saenko et al., 2004) warmed the Northwest Pacific and destabilised the permanent halocline. In contrast, sea surface temperature (SST) records from the Northwest Pacific suggest SST minima during these intervals (Harada et al., 2012; Max et al., 2012). Hence, the proposed strength in overturning circulation and its associated impact on SSTs during HS-1 and the YD seems to have been overestimated by model simulations. This would be consistent with proxy data from the deep North Pacific, which indicate no direct deep-water ventilation during the last deglaciation (Lund et al., 2011; Jaccard and Galbraith, 2013). However, anomalously young ventilation ages during HS-1 have been recently reported from a deep-sea core in the Gulf of Alaska and point to at least some regional changes of deep circulation in the Northeast Pacific Ocean (Sarnthein et al., 2013).

Pulses of enhanced North Pacific Intermediate Water ventilation

L. Max et al.

[Title Page](#)

[Abstract](#)

[Introduction](#)

[Conclusions](#)

[References](#)

[Tables](#)

[Figures](#)

[⏪](#)

[⏩](#)

[◀](#)

[▶](#)

[Back](#)

[Close](#)

[Full Screen / Esc](#)

[Printer-friendly Version](#)

[Interactive Discussion](#)

Information on changes in Northwest Pacific Intermediate Water ventilation is available from a few sediment records (1000–1300 m water depth) located at the eastern coast of Japan. At these sites, differences in radiocarbon ages between planktic and benthic foraminifers (defined as ventilation ages) are reduced during HS-1 and the YD and point to a better ventilation of NPIW (Duplessy et al., 1989; Ahagon et al., 2003; Sagawa and Ikehara, 2008). However, necessary information on ventilation changes from shallower sites in the Northwest Pacific are not available and important aspects about the mode of formation of deglacial NPIW as well as the respective roles of the Bering Sea or the Okhotsk Sea as most likely source regions of NPIW are not well known. Available studies on circulation changes from these key regions point to alternatively the Bering Sea (Horikawa et al., 2010; Rella et al., 2012) or the Okhotsk Sea (Tanaka and Takahashi, 2005) as major contributor of enhanced NPIW formation in the past. Another crucial aspect is the timing of deglacial circulation changes in the Northwest Pacific. Based on model simulations with GCMs a rapid switch and a seesaw pattern between changes in Pacific and Atlantic overturning circulation cells prevailed during the last deglaciation (Okazaki et al., 2010). However, high-resolution proxy records of millennial-scale ventilation changes in the Northwest Pacific that include the high-latitude marginal seas are still missing and impede the understanding about potential relationships and interactions between Pacific and Atlantic circulation changes during the last deglaciation.

Here we present a detailed view on deglacial Northwest Pacific circulation changes by providing new proxy data for ventilation changes derived from epibenthic $\delta^{13}\text{C}$ records in combination with a suite of new ventilation ages from the Northwest Pacific and its marginal seas (Fig. 1). From this we constrain: (1) the link between ventilation changes in the open Northwest Pacific and its marginal seas, (2) the temporal relationship of ventilation changes to variations in Atlantic Meridional Overturning Circulation (AMOC), (3) whether ventilation changes in Okhotsk Sea, Bering Sea or both represent the major source of enhanced NPIW during the last deglaciation.

2 Material and methods

2.1 Measurements of $\delta^{13}\text{C}_{\text{DIC}}$ of seawater

Modern vertical distribution of $\delta^{13}\text{C}_{\text{DIC}}$ throughout the water column was derived from two hydrocast stations proximal to the Bering Sea core SO201-2-85KL (SO201-2-67; 56°04' N, 169°14' E) and Okhotsk Sea core SO178-13-6 (LV29-84-3, 52°42' N, 144°13' E) (Fig. 1). Samples were collected during the joint German–Russian expeditions LV29 of R/V *Akademik M.A. Lavrentyev* in 2002 to the Okhotsk Sea (Biebow et al., 2002) and SO201-2 of R/V *Sonne* in 2009 to the Bering Sea (Dullo et al., 2009) via a rosette water sampling system. Water samples were poisoned with a saturated solution of HgCl_2 to stop biological activity, sealed airtight, and stored at 4 °C temperature until further treatment. Bering Sea samples were measured with a Finnigan Gas Bench II coupled to a Finnigan MAT 252 mass spectrometer for determination of stable carbon isotope ratio at the Alfred Wegener Institute in Bremerhaven (AWI). Measurements of the $\delta^{13}\text{C}_{\text{DIC}}$ from Okhotsk sea samples were carried out in the Leibniz Laboratory for Radiometric Dating and Isotope Research in Kiel, using an automated Kiel DICI-II device for CO_2 extraction and a Finnigan MAT Delta E mass spectrometer according to established procedures (Erlenkeuser et al., 1995, 1999). Results are given in δ -notation versus VPDB. The precision of $\delta^{13}\text{C}_{\text{DIC}}$ measurements based on internal laboratory standards has been reported to be better than ± 0.1 ‰ at both laboratories.

2.2 Benthic stable carbon isotope records ($\delta^{13}\text{C}$)

Stable carbon isotope records ($\delta^{13}\text{C}$) derived from tests of epibenthic foraminifera have been long documented as robust proxy to trace past variations in deep-water circulation since it is closely linked to past ambient seawater $\delta^{13}\text{C}_{\text{DIC}}$ nutrient- and oxygen levels (Belanger et al., 1981; Duplessy et al., 1984; Curry et al., 1988; Curry and Oppo, 2005). In general, high (low) $\delta^{13}\text{C}_{\text{DIC}}$ values are indicative of low (high) nutrient concentrations and associated changes in ocean circulation (Kroopnick, 1985). For stable

CPD

9, 6221–6253, 2013

Pulses of enhanced North Pacific Intermediate Water ventilation

L. Max et al.

Title Page

Abstract

Introduction

Conclusions

References

Tables

Figures

⏪

⏩

◀

▶

Back

Close

Full Screen / Esc

Printer-friendly Version

Interactive Discussion

Pulses of enhanced North Pacific Intermediate Water ventilation

L. Max et al.

[Title Page](#)

[Abstract](#)

[Introduction](#)

[Conclusions](#)

[References](#)

[Tables](#)

[Figures](#)

[⏪](#)

[⏩](#)

[◀](#)

[▶](#)

[Back](#)

[Close](#)

[Full Screen / Esc](#)

[Printer-friendly Version](#)

[Interactive Discussion](#)

isotope analysis, we only used specimens of the epibenthic species *Cibicides lobatulus* (*C. lobatulus*) from the 250–500 μm fraction. Some studies have observed a positive offset in the $\delta^{13}\text{C}$ of this species with regard to ambient bottom water for $\delta^{13}\text{C}$ at the time of sampling in other high latitude settings. However, this effect was shown to be likely caused by high seasonal variability of the ambient water $\delta^{13}\text{C}$ -signal as indicated by time-series measurements of water column $\delta^{13}\text{C}$ and according calcification of *C. lobatulus* during time intervals of maximum ventilation (Mackensen et al., 2000).

Prior to stable isotope determination, sediment samples from cores SO178-13-6 (Okhotsk Sea) and SO201-2-85KL (Western Bering Sea) (Fig. 1) were freeze-dried, wet sieved at 63 μm , dried and separated in several sub-fractions (63–150, 150–250, 250–500, > 500 μm). If possible, we picked three to five specimens per sample and restricted our selection to well-preserved specimen with visible pores, clear sutures and unfilled chambers. During some intervals with low benthic foraminiferal abundance, single specimens were used for analysis.

Samples from core SO178-13-6 were measured with a Thermo Finnigan MAT 252 isotope ratio mass spectrometer coupled to an automated KIEL II CARBO preparation device at the GEOMAR – Helmholtz Centre for Ocean Research in Kiel. Samples from core SO201-2-85KL were measured with a Thermo Finnigan MAT 253 isotope ratio mass spectrometer coupled to an automated KIEL IV CARBO preparation device at the Stable Isotope Laboratory at the AWI. Overall analytical reproducibility of laboratory standards (Solnhofen limestone) measured together with samples over one year for $\delta^{13}\text{C}$ is better than $\pm 0.06\text{‰}$ at both laboratories. Calibration was achieved via National Bureau of Standards NBS19 international standard vs. VPDB (Table 1).

2.3 X-ray fluorescence (XRF) measurements

XRF measurements were conducted on core SO178-13-6 at the Center for Marine Environmental Science (MARUM), Bremen. Each core segment was double-scanned for element analysis at 1 mA and tube voltages of 10 kV (Al, Si, S, K, Ca, Ti, Fe) and 50 kV (Ag, Cd, Sn, Te, Ba), using a sampling resolution of 1 cm and 30 s count time.

2.4 Radiocarbon dating (AMS ^{14}C)

For radiocarbon dating a sufficient amount of planktic foraminifera (*G. bulloides* and/or *Neogloboquadrina pachyderma* sinistral) was picked from the 150–250 μm size fraction. Radiocarbon dating (AMS ^{14}C) was done by BETA Analytics London, the National Ocean Science Accelerator Mass Spectrometry Facility (NOSAMS) at Woods Hole Oceanographic Institute (WHOI) as well as the Leibniz-Laboratory for Radiometric Dating and Isotope Research at Kiel University. Radiocarbon ages are given according to the convention outlined by Stuiver and Polach (1977) and Stuiver (1980) and summarized in Table 2. We applied reservoir age correction of +900 yr (Max et al., 2012) for core SO178-13-6, which is determined by a marine global average reservoir age correction of +400 yr (Reimer et al., 2009) and a local planktic reservoir age correction (ΔR) of +500 yr reported for the Okhotsk Sea environment (Kuzmin et al., 2001, 2007). All planktic radiocarbon ages were converted into calibrated 1-sigma calendar age ranges using the calibration tool Calib Rev 6.10 (Stuiver and Reimer, 1993) with the Intcal09 atmospheric calibration curve (Reimer et al., 2009). In addition to planktic ^{14}C measurements radiocarbon dating was performed on mono-specific samples of the benthic foraminifera *Uvigerina peregrina* to assess past changes in ventilation ages. Ventilation ages were calculated from raw ^{14}C age differences between co-existing planktic and benthic foraminifers (Broecker et al., 2004). In total, 26 ventilation ages were derived from a set of six sediment cores covering a depth range of approx. 600–2100 m water depth in Northwest Pacific region (Fig. 1 and Table 2). These data, together with published ventilation ages from the deep Northwest Pacific (> 2100 m water depth), are summarized in Table 3.

3 Chronology

The stratigraphy of the sediment records from the Bering Sea (SO201-2-77KL; SO201-1-85KL; SO201-2-101KL), Okhotsk Sea (LV29-114-3) and the Northwest Pacific

CPD

9, 6221–6253, 2013

Pulses of enhanced North Pacific Intermediate Water ventilation

L. Max et al.

Title Page

Abstract

Introduction

Conclusions

References

Tables

Figures

⏪

⏩

◀

▶

Back

Close

Full Screen / Esc

Printer-friendly Version

Interactive Discussion



Pulses of enhanced North Pacific Intermediate Water ventilation

L. Max et al.

Title Page

Abstract

Introduction

Conclusions

References

Tables

Figures

⏪

⏩

◀

▶

Back

Close

Full Screen / Esc

Printer-friendly Version

Interactive Discussion

(SO201-2-12KL) (Fig. 1) is presented in detail in Max et al. (2012). These records are part of a stratigraphic framework for the subarctic Northwest Pacific and its marginal seas (Riethdorf et al., 2013). In general, it is based on detailed core-to-core correlations using high-resolution XRF measurements and core logger data, further constrained by 40 planktic foraminiferal AMS ^{14}C dating's spanning the time interval of the last deglaciation. For this study, core SO178-13-6 from the Okhotsk Sea ($52^{\circ}43' \text{N}$, $144^{\circ}42' \text{E}$, 713 m water depth) was integrated via correlation of Ca intensity records (based on XRF-scanning) and AMS ^{14}C dating's to the established stratigraphic framework for the subarctic Northwest Pacific and its marginal seas as shown in Fig. 2 (Max et al., 2012).

4 Results and discussion

4.1 Modern properties of Okhotsk Sea and Bering Sea $\delta^{13}\text{C}_{\text{DIC}}$

The modern distribution of $\delta^{13}\text{C}_{\text{DIC}}$ in the water column indicates large differences between the Okhotsk Sea and Bering Sea as shown in Fig. 3. As expected, the $\delta^{13}\text{C}_{\text{DIC}}$ profile from the Okhotsk Sea shows a smooth decline of $\delta^{13}\text{C}_{\text{DIC}}$ values within the water column between 200–800 m (Fig. 3). This marks the presence of fresh, newly formed Okhotsk Sea Intermediate Water (OSIW), which spreads across the Okhotsk Sea, subsequently exported through the Kurile Straits into the Northwest Pacific. Today, the Okhotsk Sea sediment record SO178-13-6 is bathed in OSIW with $\delta^{13}\text{C}_{\text{DIC}}$ values around -0.3‰ .

In the Western Bering Sea, a large gradient in $\delta^{13}\text{C}_{\text{DIC}}$ exists around 150 m water depth, which marks the maximum in mixed layer depth of surface water mixing with underlying water masses during winter (Fig. 3). Beyond, the $\delta^{13}\text{C}_{\text{DIC}}$ values rapidly decline to -0.6 to -0.7‰ and indicate nutrient-rich, poorly ventilated water masses in the Western Bering Sea today. Low $\delta^{13}\text{C}_{\text{DIC}}$ values of ca. -0.6‰ mark the depth

interval of sediment core SO201-2-85KL and are related to the intrusion of old and nutrient-rich Pacific Deep Water at this site (Luchin et al., 1999).

4.2 Characteristics of deglacial NPIW variations and their potential source regions

We use the down-core variations in $\delta^{13}\text{C}$ and ventilation ages to assess the timing and magnitude of paleo-circulation changes in the subarctic Northwest Pacific and its marginal seas. To infer the relative timing of ventilation changes in the Western Bering Sea we compare the intermediate-depth benthic $\delta^{13}\text{C}$ record to published $^{231}\text{Pa}/^{230}\text{Th}$ data (proposed to reflect the strength of the AMOC) from the North Atlantic (McManus et al., 2004) and millennial-scale climate oscillations of Greenland (Rasmussen et al., 2006) during the last deglaciation (Fig. 4). In general, the Western Bering Sea $\delta^{13}\text{C}$ proxy data reveals millennial-scale, rapid oscillations in $\delta^{13}\text{C}$ that indicate repeated mid-depth ventilation changes. These prominent, short-term excursions in $\delta^{13}\text{C}$ are strictly opposite in sign (ventilation seesaw) compared to the North Atlantic deep circulation history of the last 20 kyr as indicated by $^{231}\text{Pa}/^{230}\text{Th}$ data (Fig. 4). Specifically, the Western Bering Sea $\delta^{13}\text{C}$ proxy data point to times of intensified ventilation of intermediate waters during HS-1 (17.5–15 kyrBP) and the YD (12.8–11.8 kyrBP) as indicated by relatively high $\delta^{13}\text{C}$ values (–0.1 to –0.2 ‰) during times when North Atlantic Deep Water (NADW) formation in the North Atlantic was significantly reduced (McManus et al., 2004). Compared to modern conditions (see also Sect. 4.1) $\delta^{13}\text{C}$ values increase by approx. (0.4–0.5 ‰) during HS-1 and YD, respectively. However, as soon as the North Atlantic deep overturning cell was re-established during the Bølling/Allerød (14.7–12.8 kyrBP) and the onset of the Holocene, ventilation of Western Bering Sea Intermediate Water diminished to modern values of approx. –0.4 to –0.7 ‰ and point to rapid changes in circulation (Fig. 4).

The deglacial pattern of Okhotsk Sea Intermediate Water ventilation resembles the mid-depth ventilation history of the Bering Sea (Fig. 5). Although the timing of changes is similar, the amplitude of changes is significantly higher in the Okhotsk Sea (up to

Pulses of enhanced North Pacific Intermediate Water ventilation

L. Max et al.

Title Page

Abstract

Introduction

Conclusions

References

Tables

Figures

⏪

⏩

◀

▶

Back

Close

Full Screen / Esc

Printer-friendly Version

Interactive Discussion



Pulses of enhanced North Pacific Intermediate Water ventilation

L. Max et al.

[Title Page](#)

[Abstract](#)

[Introduction](#)

[Conclusions](#)

[References](#)

[Tables](#)

[Figures](#)

[⏪](#)

[⏩](#)

[◀](#)

[▶](#)

[Back](#)

[Close](#)

[Full Screen / Esc](#)

[Printer-friendly Version](#)

[Interactive Discussion](#)

5 diate water level (700–1750 m water depth), Okhotsk Sea and Bering Sea ventilation
ages are low during HS-1 and YD, thus pointing to the presence of well-ventilated water
masses (Fig. 5). In general, this pattern is consistent with ventilation ages from the mid-
depth Northwest Pacific during HS-1 and YD and, like the results from $\delta^{13}\text{C}$, suggests
10 a close relationship to NPIW (Duplessy et al., 1989; Adkins and Boyle, 1997; Ahagon
et al., 2003; Sagawa and Ikehara, 2008). However, a more complex picture evolves
during the Bølling/Allerød. On the one hand, higher ventilation ages from Okhotsk Sea
core LV29-114-3 (approx. 1750 m water depth) point to a reduced vertical expansion of
freshly formed intermediate water during the Bølling/Allerød. On the other hand, there
15 is no significant change in ventilation seen from the shallowest records in the Bering
Sea (SO201-2-101; 600 m water depth) or Okhotsk Sea (SO178-13-6; 713 m water
depth) during the onset of the Bølling/Allerød. In contrast to the intermediate water
level, deep-water ventilation ages (here defined as interval deeper than 2100 m water
depth) are generally high (Murayama et al., 1992; Keigwin, 2002; Sarnthein et al., 2006;
20 Minoshima et al., 2007; Okazaki et al., 2012) and indicate persistent, old water masses
in the deep relative to the intermediate water during the last deglaciation. The largest
ventilation age difference between the intermediate and deep-water masses occurs
during HS-1 and matches the results from $\delta^{13}\text{C}$ measurements, which also indicate the
largest vertical gradient in $\delta^{13}\text{C}$ between the intermediate- and deep-water masses of
25 the Northwest Pacific during HS-1 (Fig. 5). Differences between the intermediate and
deep-water mass signatures are also visible during YD, but are less pronounced. The
opposite is the case from ca. 20–19 kyrBP and during the Bølling/Allerød as ventila-
tion ages from the intermediate and deep-water masses slightly converge, indicated by
increasing ventilation ages at the intermediate water level and decreasing deep-water
ventilation ages (Fig. 5).

In summary, during times of HS-1 and the YD the combination of benthic $\delta^{13}\text{C}$ and
ventilation ages suggests: (1) an enhanced NPIW formation and better ventilation down
to at least 1750 m water depth (but shallower than 2100 m water depth), (2) a deglacial
source of intermediate water formation within or close to the Okhotsk Sea as key re-

Pulses of enhanced North Pacific Intermediate Water ventilation

L. Max et al.

[Title Page](#)

[Abstract](#)

[Introduction](#)

[Conclusions](#)

[References](#)

[Tables](#)

[Figures](#)

[⏪](#)

[⏩](#)

[◀](#)

[▶](#)

[Back](#)

[Close](#)

[Full Screen / Esc](#)

[Printer-friendly Version](#)

[Interactive Discussion](#)

gion for millennial-scale NPIW changes (3) a more isolated deep-water that has been located deeper episodically during the last glacial termination, overlain by younger, relatively fresh intermediate water masses. This circulation is characterized by strongest vertical gradients in benthic $\delta^{13}\text{C}$ and ventilation ages in the water column between intermediate- and deep-water during HS-1 and YD. It is also in harmony with studies indicating that the abyssal North Pacific was more isolated from the atmosphere during HS-1 and did not contribute to the rise in atmospheric CO_2 during this interval (Galbraith et al., 2007). However, these results contradict the model-derived hypothesis of a switch to deep-water formation in the Northwest Pacific during HS-1 (Okazaki et al., 2010).

4.3 Implications for formation processes of expanded NPIW during HS-1

The large change in OSIW $\delta^{13}\text{C}$ values with amplitudes of 1.5‰ between HS-1 and the Bølling/Allerød provide useful information about the boundary conditions of intermediate water formation in the Northwest Pacific and points to the Okhotsk Sea as primary source for millennial-scale ventilation changes. However, it is also clear that conditions must have been substantially different from those of modern OSIW formation. Under present conditions, intermediate water masses are a blend of surface water and old Pacific Deep Water, which enters the Okhotsk Sea basin through the deepest sills of the Kurile Islands (mainly through Kruzenshtern Strait, ca. 1760 m water depth) (Talley and Roemmich, 1991). Due to the intrusion of old and nutrient-enriched Pacific Deep Water, modern OSIW is marked by relatively high nutrient concentrations and low $\delta^{13}\text{C}$ values of 0 to -0.3‰ (see also Fig. 3). Thermodynamic effects due to reduced SST and reduced biological productivity cannot solely explain the extremely high $\delta^{13}\text{C}$ values during HS-1. Thus, we speculate that the main source of enhanced OSIW during HS-1 and the YD was shifted from old Pacific deep-water to relatively young and nutrient-depleted surface water masses, which flowed from the North Pacific into the Okhotsk Sea. This is in line with the presence of young water masses down to about 1750 m water depth (i.e. Okhotsk Sea core LV29-114-3) during HS-1. Once the inten-

sified OSIW formation flushed the Okhotsk Sea up to the deepest sills, the inflow of old and $\delta^{13}\text{C}$ -depleted deep-water masses from the North Pacific into the Okhotsk Sea basin must have been significantly hampered or even blocked during HS-1 or the YD.

4.4 Relation of deglacial NPIW patterns to changes in meridional overturning circulation and atmospheric pressure regimes

The implication of a strengthened shallow meridional overturning in the North Pacific in response to AMOC reductions during HS-1 and YD agrees with results from GCM simulations, which predict enhanced ventilation of NPIW down to approx. 2000 m water depth during these intervals (Chikamoto et al., 2012). However, our results do not corroborate model simulations that argue for a more fundamental switch to Pacific deep-water formation down to approx. 3000 m water depth (Okazaki et al., 2010). In the first case, the largest cooling trend appears during HS-1 in the GCM simulations in the Western North Pacific in association with severe cooling of the overlying atmosphere in the Northern Hemisphere and intensification of the Aleutian Low, thus promoting sea-ice expansion and enhanced mid-depth circulation. In the latter case, the establishment of a deep PMOC is physically coupled to a strengthened northeastward upper-ocean heat and salinity transport via the North Pacific Current, thereby warming the Northwest Pacific during HS-1 and YD (Saenko et al., 2004; Krebs and Timmermann, 2007; Okazaki et al., 2010). SST records in combination with sea-ice reconstructions provide no evidence of surface warming during HS-1 and YD in the Northwest Pacific (Fig. 5), rendering this scenario unlikely (Max et al., 2012). We thus assume that millennial-scale enhancements in NPIW formation during the last deglaciation can be explained by mechanisms that involve intensified processes of dense water formation in the Okhotsk Sea, which are in turn coupled to more intense OSIW formation under colder conditions during HS-1 and YD.

In addition, our results provide clues for future changes in marine biogeochemistry. Past changes in mid-depth oxygen concentrations in the Northwest Pacific are often related to a substantial weakening of NPIW and its consequences in favouring the ex-

Pulses of enhanced North Pacific Intermediate Water ventilation

L. Max et al.

Title Page

Abstract

Introduction

Conclusions

References

Tables

Figures

⏪

⏩

◀

▶

Back

Close

Full Screen / Esc

Printer-friendly Version

Interactive Discussion



Pulses of enhanced North Pacific Intermediate Water ventilation

L. Max et al.

Title Page

Abstract

Introduction

Conclusions

References

Tables

Figures



Back

Close

Full Screen / Esc

Printer-friendly Version

Interactive Discussion



and deep-water records provides no evidence for a deep-water formation in the Northwest Pacific during HS-1 and YD.

2. The deglacial source of enhanced North Pacific Intermediate Water formation during cold events of HS-1 and YD was very probably within the Okhotsk Sea and coupled to processes of improved OSIW formation, which acted as pacemaker for NPIW changes. It seems likely that times of enhanced ventilation of the Bering Sea are coupled to more rigorous formation of NPIW.
3. The strengthening of NPIW and shallow overturning during HS-1 and YD would argue for a deepening of the nutricline within the Northwest Pacific. A mode of intensified shallow overturning through enhanced NPIW ventilation in the North Pacific might have reduced the upwelling of old, nutrient and CO₂-enriched Pacific deep-water masses and subsequent exchange with the atmosphere.

Acknowledgements. We gratefully acknowledge the Master and crew of R/V *Sonne* cruises SO178, SO201-2 and R/V *Akademik M.A. Lavrentyev* (LV29) and thank for their professional support on-board. We express our thanks to L. Schönborn and G. Meyer for running the mass spectrometer laboratory at AWI stable isotope lab. Samples from this study were collected during German – Russian projects KOMEX-SONNE (03G0178A), KOMEX II (03G0535A), KALMAR (03G0672B and 03G0672A) and funded by the German Federal Ministry of Education and Research (BMBF). The Helmholtz Climate Initiative REKLIM (Regional climate change) funded this study.

References

Adkins, J. F. and Boyle, E. A.: Changing atmospheric delta C-14 and the record of deep water paleoventilation ages, *Paleoceanography*, 12, 337–344, 1997.

Ahagon, N., Ohkushi, K., Uchida, M., and Mishima, T.: Mid-depth circulation in the Northwest Pacific during the last deglaciation: evidence from foraminiferal radiocarbon ages, *Geophys. Res. Lett.*, 30, 2097, doi:10.1029/2003GL018287, 2003.

Pulses of enhanced North Pacific Intermediate Water ventilation

L. Max et al.

[Title Page](#)

[Abstract](#)

[Introduction](#)

[Conclusions](#)

[References](#)

[Tables](#)

[Figures](#)

[⏪](#)

[⏩](#)

[◀](#)

[▶](#)

[Back](#)

[Close](#)

[Full Screen / Esc](#)

[Printer-friendly Version](#)

[Interactive Discussion](#)

- Behl, R. J. and Kennett, J. P.: Brief interstadial events in the Santa Barbara basin, NE Pacific, during the past 60 kyr, *Nature*, 379, 243–246, 1996.
- Belanger, P. E., Curry, W. B., and Matthews, R. K.: Core-top evaluation of benthic foraminiferal isotopic-ratios for paleo-oceanographic interpretations, *Palaeogeogr. Palaeoecol.*, 33, 205–220, 1981.
- Biebow, N., Kulinich, R., and Baranov, B.: KOMEX II, Kurile Okhotsk Sea Marine Experiment: cruise report RV *Akademik M. A. Lavrentyev* cruise 29, leg 1 and leg 2, in: GEOMAR-Report 110, edited by: Biebow, N., Kulinich, R., and Baranov, B., Leibniz Institute of Marine Sciences, Kiel, 2002.
- Broecker, W., Barker, S., Clark, E., Hajdas, I., Bonani, G., and Stott, L.: Ventilation of the glacial deep Pacific Ocean, *Science*, 306, 1169–1172, 2004.
- Cartapanis, O., Tachikawa, K., and Bard, E.: Northeastern Pacific oxygen minimum zone variability over the past 70 kyr: impact of biological production and oceanic ventilation, *Paleoceanography*, 26, PA4208, doi:10.1029/2011PA002126, 2011.
- Chikamoto, M. O., Menviel, L., Abe-Ouchi, A., Ohgaito, R., Timmermann, A., Okazaki, Y., Harada, N., Oka, A., and Mouchet, A.: Variability in North Pacific Intermediate and Deep Water ventilation during Heinrich events in two coupled climate models, *Deep-Sea Res. Pt. II*, 61–64, 114–126, 2012.
- Cook, M. S., Keigwin, L. D., and Sancetta, C. A.: The deglacial history of surface and intermediate water of the Bering Sea, *Deep-Sea Res. Pt. II*, 52, 2163–2173, 2005.
- Curry, W. B. and Oppo, D. W.: Glacial water mass geometry and the distribution of $\delta^{13}\text{C}$ of Sigma CO_2 in the Western Atlantic Ocean, *Paleoceanography*, 20, PA1017, doi:10.1029/2004PA001021, 2005.
- Curry, W. B., Duplessy, J. C., Labeyrie, L. D., and Shackleton, N. J.: Changes in the distribution of $\delta^{13}\text{C}$ of deep water TCO_2 between the last glaciation and the Holocene, *Paleoceanography*, 3, 317–341, 1988.
- Dullo, W. C., Baranov, B., and van den Bogaard, C.: FS *Sonne* Fahrtbericht/Cruise Report SO201-2 KALMAR, Busan/Korea–Tomakomai/Japan, 30 August–8 October 2009, in: IFM-GEOMAR Report 35, edited by: van den Bogaard, C., Leibniz Institute of Marine Sciences, Kiel, 2009.
- Duplessy, J. C., Shackleton, N. J., Matthews, R. K., Prell, W., Ruddiman, W. F., Caralp, M., and Hendy, C. H.: C-13 record of benthic foraminifera in the last interglacial ocean – implications

Pulses of enhanced North Pacific Intermediate Water ventilation

L. Max et al.

[Title Page](#)

[Abstract](#)

[Introduction](#)

[Conclusions](#)

[References](#)

[Tables](#)

[Figures](#)

[⏪](#)

[⏩](#)

[◀](#)

[▶](#)

[Back](#)

[Close](#)

[Full Screen / Esc](#)

[Printer-friendly Version](#)

[Interactive Discussion](#)

- Keigwin, L. D.: Glacial-age hydrography of the far Northwest Pacific Ocean, *Paleoceanography*, 13, 323–339, 1998.
- Keigwin, L. D.: Late Pleistocene–Holocene paleoceanography and ventilation of the Gulf of California, *J. Oceanogr.*, 58, 421–432, 2002.
- 5 Kim, S., Khim, B. K., Uchida, M., Itaki, T., and Tada, R.: Millennial-scale paleoceanographic events and implications for the intermediate-water ventilation in the northern slope area of the Bering Sea during the last 71 kyr, *Global Planet. Change*, 79, 89–98, 2011.
- Krebs, U. and Timmermann, A.: Tropical air–sea interactions accelerate the recovery of the atlantic meridional overturning circulation after a major shutdown, *J. Climate*, 20, 4940–4956, 10 2007.
- Kroopnick, P. M.: The distribution of C-13 of sigma-CO₂ in the world oceans, *Deep-Sea Res. Pt. I*, 32, 57–84, 1985.
- Kuzmin, Y. V., Burr, G. S., and Jull, A. J. T.: Radiocarbon reservoir correction ages in the Peter the Great Gulf, Sea of Japan, and eastern coast of the Kunashir, Southern Kuriles (North-western Pacific), *Radiocarbon*, 43, 477–481, 2001.
- 15 Kuzmin, Y. V., Burr, G. S., Gorbunov, S. V., Rakov, V. A., and Razjigaeva, N. G.: A tale of two seas: reservoir age correction values (R , ΔR) for the Sakhalin Island (Sea of Japan and Okhotsk Sea), *Nucl. Instrum. Meth. B*, 259, 460–462, 2007.
- Luchin, V. A., Menovshchikow, V. A., Lavrentiev, V. M., and Reed, R. K.: Thermohaline structure and water masses in the Bering Sea, in: *Dynamics of the Bering Sea*, edited by: Loughlin, T. R. and Ohtani, K., University of Alaska Grant, Fairbanks, 61–92, 1999.
- 20 Lund, D. C., Mix, A. C., and Southon, J.: Increased ventilation age of the deep Northeast Pacific Ocean during the last deglaciation, *Nat. Geosci.*, 4, 771–774, 2011.
- Mackensen, A., Schumacher, S., Radke, J., and Schmidt, D. N.: Microhabitat preferences and stable carbon isotopes of endobenthic foraminifera: clue to quantitative reconstruction of oceanic new production?, *Mar. Micropaleontol.*, 40, 233–258, 2000.
- 25 Max, L., Riethdorf, J. R., Tiedemann, R., Smirnova, M., Lembke-Jene, L., Fahl, K., Nurnberg, D., Matul, A., and Mollenhauer, G.: Sea surface temperature variability and sea-ice extent in the subarctic Northwest Pacific during the past 15 000 years, *Paleoceanography*, 27, PA3213, doi:10.1029/2012PA002292, 2012.
- 30 McManus, J. F., Francois, R., Gherardi, J. M., Keigwin, L. D., and Brown-Leger, S.: Collapse and rapid resumption of Atlantic meridional circulation linked to deglacial climate changes, *Nature*, 428, 834–837, 2004.

Pulses of enhanced North Pacific Intermediate Water ventilation

L. Max et al.

[Title Page](#)

[Abstract](#)

[Introduction](#)

[Conclusions](#)

[References](#)

[Tables](#)

[Figures](#)

[⏪](#)

[⏩](#)

[◀](#)

[▶](#)

[Back](#)

[Close](#)

[Full Screen / Esc](#)

[Printer-friendly Version](#)

[Interactive Discussion](#)

- Menviel, L., Timmermann, A., Timm, O. E., Mouchet, A., Abe-Ouchi, A., Chikamoto, M. O., Harada, N., Ohgaito, R., and Okazaki, Y.: Removing the North Pacific halocline: effects on global climate, ocean circulation and the carbon cycle, *Deep-Sea Res. Pt. II*, 61–64, 106–113, 2012.
- 5 Mikolajewicz, U., Crowley, T. J., Schiller, A., and Voss, R.: Modelling teleconnections between the North Atlantic and North Pacific during the Younger Dryas, *Nature*, 387, 384–387, 1997.
- Minoshima, K., Kawahata, H., Irino, T., Ikehara, K., Aoki, K., Uchida, M., Yoneda, M., and Shibata, Y.: Deep water ventilation in the Northwestern North Pacific during the last deglaciation and the early Holocene (15–5 cal. kyr BP) based on AMS C-14 dating, *Nucl. Instrum. Meth. B*, 10 259, 448–452, 2007.
- Murayama, M., Taira, A., Iwakura, H., Matsumoto, E., and Nakamura, T.: Northwest Pacific deep water ventilation rate during the past 35 000 years with the AMS 14C foraminifera ages, *Summaries of Researchers Using AMS at Nagoya University*, vol. 3, Nagoya University Center for Chronological Research, Nagoya, Japan, 114–121, 1992.
- 15 Okazaki, Y., Timmermann, A., Menviel, L., Harada, N., Abe-Ouchi, A., Chikamoto, M. O., Mouchet, A., and Asahi, H.: Deepwater formation in the North Pacific during the Last Glacial termination, *Science*, 329, 200–204, 2010.
- Okazaki, Y., Sagawa, T., Asahi, H., Horikawa, K., and Onodera, J.: Ventilation changes in the Western North Pacific since the last glacial period, *Clim. Past*, 8, 17–24, doi:10.5194/cp-8-17-2012, 2012.
- 20 Okumura, Y. M., Deser, C., Hu, A., Timmermann, A., and Xie, S. P.: North Pacific climate response to freshwater forcing in the Subarctic North Atlantic: oceanic and atmospheric pathways, *J. Climate*, 22, 1424–1445, 2009.
- Rasmussen, S. O., Andersen, K. K., Svensson, A. M., Steffensen, J. P., Vinther, B. M., Clausen, H. B., Siggaard-Andersen, M. L., Johnsen, S. J., Larsen, L. B., Dahl-Jensen, D., Bigler, M., Rothlisberger, R., Fischer, H., Goto-Azuma, K., Hansson, M. E., and Ruth, U.: A new Greenland ice core chronology for the last glacial termination, *J. Geophys. Res.-Atmos.*, 111, D06102, doi:10.1029/2005JD006079, 2006.
- 25 Reimer, P. J., Baillie, M. G. L., Bard, E., Bayliss, A., Beck, J. W., Blackwell, P. G., Ramsey, C. B., Buck, C. E., Burr, G. S., Edwards, R. L., Friedrich, M., Grootes, P. M., Guilderson, T. P., Hajdas, I., Heaton, T. J., Hogg, A. G., Hughen, K. A., Kaiser, K. F., Kromer, B., McCormac, F. G., Manning, S. W., Reimer, R. W., Richards, D. A., Southon, J. R., Talamo, S., Turney, C. S. M.,

**Pulses of enhanced
North Pacific
Intermediate Water
ventilation**

L. Max et al.

[Title Page](#)[Abstract](#)[Introduction](#)[Conclusions](#)[References](#)[Tables](#)[Figures](#)[⏪](#)[⏩](#)[◀](#)[▶](#)[Back](#)[Close](#)[Full Screen / Esc](#)[Printer-friendly Version](#)[Interactive Discussion](#)

- van der Plicht, J., and Weyhenmeyer, C. E.: Intcal09 and Marine09 radiocarbon age calibration curves, 0–50 000 years cal. BP, *Radiocarbon*, 51, 1111–1150, 2009.
- Rella, S. F., Tada, R., Nagashima, K., Ikehara, M., Itaki, T., Ohkushi, K., Sakamoto, T., Harada, N., and Uchida, M.: Abrupt changes of intermediate water properties on the north-eastern slope of the Bering Sea during the last glacial and deglacial period, *Paleoceanography*, 27, PA3203, doi:10.1029/2011PA002205, 2012.
- 5 Riethdorf, J.-R., Nürnberg, D., Max, L., Tiedemann, R., Gorbarenko, S. A., and Malakhov, M. I.: Millennial-scale variability of marine productivity and terrigenous matter supply in the western Bering Sea over the past 180 kyr, *Clim. Past*, 9, 1345–1373, doi:10.5194/cp-9-1345-2013, 2013.
- 10 Saenko, O. A., Schmittner, A., and Weaver, A. J.: The Atlantic–Pacific seesaw, *J. Climate*, 17, 2033–2038, 2004.
- Sagawa, T. and Ikehara, K.: Intermediate water ventilation change in the subarctic Northwest Pacific during the last deglaciation, *Geophys. Res. Lett.*, 35, L24702, doi:10.1029/2008GL035133, 2008.
- 15 Sarnthein, M., Kiefer, T., Grootes, P. M., Elderfield, H., and Erlenkeuser, H.: Warmings in the far Northwestern Pacific promoted pre-Clovis immigration to America during Heinrich event 1, *Geology*, 34, 141–144, 2006.
- Sarnthein, M., Schneider, B., and Grootes, P. M.: Peak glacial ^{14}C ventilation ages suggest major draw-down of carbon into the abyssal ocean, *Clim. Past Discuss.*, 9, 925–965, doi:10.5194/cpd-9-925-2013, 2013.
- 20 Schmittner, A., Galbraith, E. D., Hostetler, S. W., Pedersen, T. F., and Zhang, R.: Large fluctuations of dissolved oxygen in the Indian and Pacific oceans during Dansgaard–Oeschger oscillations caused by variations of North Atlantic Deep Water subduction, *Paleoceanography*, 22, PA3207, doi:10.1029/2006PA001384, 2007.
- 25 Shcherbina, A. Y., Talley, L. D., and Rudnick, D. L.: Direct observations of North Pacific ventilation: brine rejection in the Okhotsk Sea, *Science*, 302, 1952–1955, 2003.
- Stuiver, M.: Workshop on C-14 data reporting, *Radiocarbon*, 22, 964–966, 1980.
- Stuiver, M. and Polach, H. A.: Reporting of C-14 data – discussion, *Radiocarbon*, 19, 355–363, 1977.
- 30 Stuiver, M. and Reimer, P. J.: Extended C-14 data-base and revised calib 3.0 C-14 age calibration program, *Radiocarbon*, 35, 215–230, 1993.

Pulses of enhanced North Pacific Intermediate Water ventilation

L. Max et al.

[Title Page](#)

[Abstract](#)

[Introduction](#)

[Conclusions](#)

[References](#)

[Tables](#)

[Figures](#)

[⏪](#)

[⏩](#)

[◀](#)

[▶](#)

[Back](#)

[Close](#)

[Full Screen / Esc](#)

[Printer-friendly Version](#)

[Interactive Discussion](#)



- Talley, L. D.: Distribution and formation of North Pacific Intermediate Water, *J. Phys. Oceanogr.*, 23, 517–537, 1993.
- Talley, L. D. and Roemmich, D.: A tribute to Reid, J. L. in recognition of 40 years of contributions to oceanography, *Deep-Sea Res. Pt. I*, 38, R7–R11, 1991.
- 5 Talley, L. D., Reid, J. L., and Robbins, P. E.: Data-based meridional overturning streamfunctions for the global ocean, *J. Climate*, 16, 3213–3226, 2003.
- Tanaka, S. and Takahashi, K.: Late Quaternary paleoceanographic changes in the Bering Sea and the Western Subarctic Pacific based on radiolarian assemblages, *Deep-Sea Res. Pt. II*, 52, 2131–2149, 2005.
- 10 Warner, M. J., Bullister, J. L., Wisegarver, D. P., Gammon, R. H., and Weiss, R. F.: Basin-wide distributions of chlorofluorocarbons CFC-11 and CFC-12 in the North Pacific: 1985–1989, *J. Geophys. Res.-Oceans*, 101, 20525–20542, 1996.
- Warren, B. A.: Why is no deep-water formed in the North Pacific, *J. Mar. Res.*, 41, 327–347, 1983.
- 15 Yasuda, I.: The origin of the North Pacific Intermediate Water, *J. Geophys. Res.-Oceans*, 102, 893–909, 1997.

Table 1. Stable isotope measurement results ($\delta^{18}\text{O}$; $\delta^{13}\text{C}$) from epibenthic foraminifera *Cibicides lobatulus*.

Core:	Core Depth (cm)	Age (kyrBP)	$\delta^{18}\text{O}$ (‰PDB)	$\delta^{13}\text{C}$ (‰PDB)
SO201-2-85KL (Western Bering Sea)	43	11.12	3.440	-0.500
	45	11.23	3.288	-0.350
	50	11.50	3.117	-0.424
	53	11.79	3.360	-0.230
	55	12.14	3.387	-0.200
	60	13.01	3.461	-0.349
	63	13.29	3.323	-0.388
	80	14.76	3.307	-0.428
	81	14.83	3.670	-0.056
	85	15.13	3.481	-0.185
	95	15.96	3.988	-0.125
	100	16.45	4.536	-0.034
	103	16.75	3.640	-0.210
	105	16.94	4.231	-0.035
	110	17.44	3.256	-0.441
	113	17.73	3.960	-0.260
	115	17.93	3.817	-0.401
	120	18.42	4.121	-0.335
	123	18.72	3.930	-0.450
125	18.91	3.965	-0.425	
130	19.41	3.839	-0.232	
131	19.51	3.864	-0.227	
133	19.70	3.900	-0.210	
SO178-13-6 (Okhotsk Sea)	1767.5	11.551	3.74	-0.33
	1772.5	11.584	3.45	-0.27
	1822.5	11.915	3.59	0.12
	1842.5	12.048	3.48	0.27
	1857.5	12.154	3.59	0.48
	1870.5	12.334	3.66	0.15
	1885.5	12.542	3.38	0.64
	1912.5	12.915	3.43	0.48
	1917.5	12.984	3.22	0.16
	1922.5	13.053	3.39	0.04
	1937.5	13.261	3.26	-0.67
	1972.5	14.506	4.07	-0.44
	2087.5	14.95	3.1	0.81
	2092.5	15.06	3.05	0.28
	2157.5	15.433	3.81	0.29
	2162.5	15.495	4.04	0.04
	2177.5	15.684	4.05	0.42
	2187.5	15.809	3.82	0.21
	2202.5	15.997	3.88	0.12
	2242.5	16.5	3.9	0.46
	2247.5	16.562	3.81	0.08
	2252.5	16.611	3.86	0.11
	2272.5	16.717	3.78	0.21
2277.5	16.744	3.88	0.31	
2292.5	16.824	3.64	0.48	
2297.5	16.85	4.12	0.48	
2307.5	16.904	3.75	0.66	
2317.5	16.957	3.11	-0.19	
SO178-13-6 (Okhotsk Sea)	2327.5	17.01	3.94	0.21
	2342.5	17.09	3.99	0.27

Pulses of enhanced North Pacific Intermediate Water ventilation

L. Max et al.

Title Page

Abstract Introduction

Conclusions References

Tables Figures

⏪ ⏩

◀ ▶

Back Close

Full Screen / Esc

Printer-friendly Version

Interactive Discussion



Table 2. AMS ^{14}C ages of the sediment records with calibrated calendar age $\pm 1\sigma$ (yr) and applied reservoir age correction used in this study. Asterisks mark AMS ^{14}C ages derived from Max et al. (2012).

Laboratory number	Sediment core	Core depth (cm)	Species	Conventional radiocarbon age (yr)	Calendar age $\pm 1\sigma$ (yr)	Reservoir age (yr)
OS-85655*	SO201-2-12KL	210–211	N.pachyderma sin.	9390 \pm 40	9484–9527	900
KIA44680*		295–296	N.pachyderma sin.	10 570 \pm 50	11 080–11 191	900
OS-87895*		340–341	N.pachyderma sin.	10 800 \pm 65	11 231–11 368	900
OS-88040		340–341	Uvigerina peregrina	11 750 \pm 50	–	–
OS-92047*		508–509	N.pachyderma sin.	12 500 \pm 50	13 340–13 498	900
OS-92050		508–509	Uvigerina peregrina	13 500 \pm 55	–	–
OS-87891*		550–551	N.pachyderma sin.	12 900 \pm 50	13 782–13 918	900
OS-87880		550–551	Uvigerina peregrina	13 850 \pm 50	–	–
OS-87902*		610–611	N.pachyderma sin.	13 350 \pm 65	14 219–14 752	900
OS-92150*		695–696	N.pachyderma sin.	13 900 \pm 55	15 227–15 872	900
OS-104953	LV29-114-3	695–696	Uvigerina peregrina	15 300 \pm 95	–	–
KIA44682*		820–821	N.pachyderma sin.	16 160 \pm 80	18 491–18 666	900
KIA44683*		875–876	N.pachyderma sin.	17 090 \pm 90	19 254–19 457	900
OS-104797		7–8	N.pachyderma sin.	1 730 \pm 35	695–765	900
OS-104961		102–103	N.pachyderma sin.	5 740 \pm 50	5 483–5 643	900
transferred age*		108–109	N.pachyderma sin.	5 850 \pm 60	5 607–5 730	900
OS-88042*		162–163	N.pachyderma sin.	8 320 \pm 40	8 236–8 310	900
KIA30864*		197–198	N.pachyderma sin.	9 630 \pm 50	9 764–10 067	900
OS-104963		197–198	Uvigerina peregrina	10 450 \pm 70	–	–
KIA30863*		232–233	N.pachyderma sin.	10 465 \pm 50	10 808–11 080	900
OS-104964	232–233	Uvigerina peregrina	11 200 \pm 75	–	–	
KIA30867*	272–273	N.pachyderma sin.	12 290 \pm 55	13 164–13 308	900	
OS-104796	272–273	Uvigerina peregrina	12 900 \pm 85	–	–	
KIA30865*	292–293	N.pachyderma sin.	13 180 \pm 60	13 960–14 457	900	
OS-104965	292–293	Uvigerina peregrina	14 000 \pm 95	–	–	
KIA30868*	317–318	N.pachyderma sin.	14 400 \pm 80	16 538–16 827	900	
OS-105415	317–318	Uvigerina peregrina	14 750 \pm 130	–	–	
KIA30866*	352–353	N.pachyderma sin.	15 130 \pm 80	17 117–17 497	900	
OS-104966	352–353	Uvigerina peregrina	16 600 \pm 120	–	–	
KIA30872	SO178-13-6	1682–1683	N.pachyderma sin.	10 560 \pm 50	10 874–11 183	900
KIA30869		2072–2073	N.pachyderma sin.	13 390 \pm 100	14 467–14 917	900
Beta-324995		2072–2073	mixed benthos	13 760 \pm 60	–	–
UCIAMS109675		2250–2251	N.pachyderma sin.	14 420 \pm 45	16 446–16 893	900
Beta-324996		2250–2251	mixed benthos	14 580 \pm 60	–	–
UCIAMS109674		2342–2343	N.pachyderma sin.	15 090 \pm 60	17 093–17 443	900
Beta-324997		2342–2343	mixed benthos	15 470 \pm 60	–	–
OS-85658*		115–116	N.pachyderma sin.	10 450 \pm 40	11 174–11 222	700
OS-85660		115–116	Uvigerina peregrina	11 650 \pm 45	–	–
OS-90700*		155–156	N.pachyderma sin.	11 500 \pm 50	12 606–12 731	700
OS-104954	155–156	Uvigerina peregrina	13 000 \pm 70	–	–	
OS-85664*	180–181	N.pachyderma sin.	13 200 \pm 45	14 501–14 945	700	
OS-85670	180–181	Uvigerina peregrina	14 450 \pm 85	–	–	
OS-85665*	SO201-2-85KL	26–27	N.pachyderma sin.	9950 \pm 40	10 378–10 507	700
OS-104759		43–44	N.pachyderma sin.	10 450 \pm 55	11 155–11 234	700
OS-105429		43–44	Uvigerina peregrina	11 250 \pm 110	–	–
OS-85669*		60–61	N.pachyderma sin.	11 950 \pm 45	13 104–13 217	700
KIA42232*		70–71	N.pachyderma sin.	12 620 \pm 90	13 665–13 887	700
OS-104959		93–94	N.pachyderma sin.	13 850 \pm 80	15 803–15 822	700
OS-104757		93–94	Uvigerina peregrina	14 050 \pm 80	–	–
OS-87890*		135–136	N.pachyderma sin.	17 350 \pm 65	19 575–19 895	700
Beta-325004		135–136	mixed benthos	19 210 \pm 90	–	–
KIA42233*		155–156	N.pachyderma sin.	20 720 \pm 160	23 706–24 194	700

Pulses of enhanced North Pacific Intermediate Water ventilation

L. Max et al.

[Title Page](#)

[Abstract](#) [Introduction](#)

[Conclusions](#) [References](#)

[Tables](#) [Figures](#)

[◀](#) [▶](#)

[◀](#) [▶](#)

[Back](#) [Close](#)

[Full Screen / Esc](#)

[Printer-friendly Version](#)

[Interactive Discussion](#)



Pulses of enhanced North Pacific Intermediate Water ventilation

L. Max et al.

Table 2. Continued.

Laboratory number	Sediment core	Core depth (cm)	Species	Conventional radiocarbon age (yr)	Calendar age $\pm 1\sigma$ (yr)	Reservoir age (yr)
OS-87887*	SO201-2-101KL	10–11	<i>N.pachyderma</i> sin.	12 600 \pm 55	13 686–13 838	700
OS-104795		10–11	<i>Uvigerina peregrina</i>	12 850 \pm 95	–	–
OS-88041*		90–91	<i>N.pachyderma</i> sin.	14 950 \pm 60	17 165–17 506	700
OS-104960		90–91	<i>Uvigerina peregrina</i>	16 800 \pm 130	–	–
KIA42229	SO202-18-6	110–111	<i>N.pachyderma</i> sin.	17 310 \pm 120	19 541–19 919	700
KIA43068*		110–111	<i>Uvigerina peregrina</i>	18 630 \pm 200	–	–
OS-85756		415–417.5	<i>N.pachyderma</i> sin.	10 850 \pm 25	11 760–11 957	700
OS-90698		415–417.5	mixed benthos	11 300 \pm 50	–	–
OS-96111		432–434.5	<i>N.pachyderma</i> sin.	10 950 \pm 55	11 827–12 102	700
OS-96112		432–434.5	mixed benthos	11 550 \pm 40	–	–
OS-94120		512–514.5	<i>N.pachyderma</i> sin.	11 150 \pm 65	12 216–12 529	700
OS-96034		512–514.5	mixed benthos	11 800 \pm 60	–	–
OS-96095		592–594.5	<i>N.pachyderma</i> sin.	11 850 \pm 60	12 942–13 126	700
OS-96035		592–594.5	mixed benthos	12 300 \pm 80	–	–

[Title Page](#)
[Abstract](#)
[Introduction](#)
[Conclusions](#)
[References](#)
[Tables](#)
[Figures](#)
[Back](#)
[Close](#)
[Full Screen / Esc](#)
[Printer-friendly Version](#)
[Interactive Discussion](#)

Table 3. Radiocarbon measurements on paired benthic/planktic foraminiferas (ventilation ages) from NW-Pacific sediment cores. Ventilation ages are given in yr and era is indicated by LGM, HS-1, B/A and Holocene, respectively.

Core	Water depth (m)	Core depth (cm)	Planktic ¹⁴ C-age (yr)	Benthic ¹⁴ C-age (yr)	Calendar age (kyr BP)*	B-P age (yr)	Error ±1-Sigma (yr)	Era	Reference
Bering Sea (intermediate)									
SO201-2-101KL	630	10	12 600 ± 55	12 850 ± 95	13.56	250	150	B/A	this study
SO201-2-101KL	630	90	14 950 ± 60	16 800 ± 130	17.25	1850	190	HS-1	
SO201-2-101KL	630	110	17 310 ± 120	18 630 ± 200	19.73	1350	320	LGM	
SO201-2-85KL									
SO201-2-85KL	968	43	10 450 ± 55	11 250 ± 110	11.20	800	165	Holocene	this study
SO201-2-85KL	968	93	13 850 ± 80	14 050 ± 80	15.80	200	160	HS-1	
SO201-2-85KL	968	135	17 350 ± 65	19 210 ± 90	19.90	1860	155	LGM	
SO202-18-6									
SO202-18-6	1100	415–417.5	10 850 ± 25	11 300 ± 50	11.80	450	75	YD	this study
SO202-18-6	1100	432–434.5	10 950 ± 55	11 550 ± 40	12.05	600	115	YD	
SO202-18-6	1100	512–514.5	11 150 ± 65	11 800 ± 60	12.35	650	115	YD	
SO202-18-6	1100	592–594.5	11 850 ± 60	12 300 ± 80	12.98	450	140	YD	
Okhotsk Sea (intermediate)									
SO178-13-6	713	2072.5	13 390 ± 100	13 760 ± 60	14.70	370	160	B/A	this study
SO178-13-6	713	2250.5	14 420 ± 45	14 580 ± 60	16.60	160	160	HS-1	
SO178-13-6	713	2342.5	15 090 ± 60	15 470 ± 60	17.09	380	160	HS-1	
LV29-114-3									
LV29-114-3	1765	197	9630 ± 50	10 450 ± 70	9.90	820	120	Holocene	this study
LV29-114-3	1765	232	10 465 ± 50	11 200 ± 75	10.90	735	125	Holocene	
LV29-114-3	1765	272	12 290 ± 60	12 900 ± 85	13.25	610	145	B/A	
LV29-114-3	1765	292	13 180 ± 60	14 000 ± 95	14.30	820	155	B/A	this study
LV29-114-3	1765	317	14 400 ± 80	14 750 ± 130	16.50	350	210	HS-1	
LV29-114-3	1765	352	15 130 ± 80	16 600 ± 120	17.12	1470	200		
North Pacific (deep)									
SO201-2-12KL	2145	340	10 800 ± 65	11 750 ± 50	11.31	950	115	Holocene	this study
SO201-2-12KL	2145	508	12 500 ± 50	13 500 ± 55	13.38	1000	105	B/A	
SO201-2-12KL	2145	550	12 900 ± 50	13 850 ± 50	13.79	950	100	B/A	
SO201-2-12KL	2145	695	13 900 ± 55	15 300 ± 95	15.90	1400	150	HS-1	this study
KR02-15 PC6									
KR02-15 PC6	2215	539.2	10 610 ± 90	11 840 ± 60	10.91	1230	150	Holocene	Minoshima
KR02-15 PC6	2215	555.1	10 860 ± 70	12 490 ± 110	11.46	1630	180	Holocene	et al. (2007)
KR02-15 PC6	2215	575.6	13 470 ± 70	14 500 ± 120	14.80	1030	190	B/A	

* Recalculated with a constant reservoir age correction of 700 yr for the Bering Sea and 900 yr for the NW-Pacific and Okhotsk Sea, respectively.

Pulses of enhanced North Pacific Intermediate Water ventilation

L. Max et al.

Title Page

Abstract

Introduction

Conclusions

References

Tables

Figures

⏪

⏩

◀

▶

Back

Close

Full Screen / Esc

Printer-friendly Version

Interactive Discussion

Table 3. Continued.

Core	Water depth (m)	Core depth (cm)	Planktic ¹⁴ C-age (yr)	Benthic ¹⁴ C-age (yr)	Calendar age (kyr BP)*	B-P age (yr)	Error ±1-Sigma (yr)	Era	Reference	
KT89-18-P4	2700	185–190	9800 ± 133	11 140 ± 159	10.00	1340	292	Holocene	Murayama et al. (1992)	
KT89-18-P4	2700	200–204	10 692 ± 108	12 034 ± 94	11.20	1342	202	Holocene		
KT89-18-P4	2700	236–240	11 622 ± 101	13 350 ± 238	12.60	1728	339	YD		
KT89-18-P4	2700	268–272	12 450 ± 91	14 423 ± 237	13.30	1973	328	B/A		
KT89-18-P4	2700	338–342	13 447 ± 113	14 681 ± 103	14.60	1234	216	B/A		
KT89-18-P4	2700	449–453	17 275 ± 478	19 267 ± 557	19.50	1992	1035	LGM		
KT89-18-P4	2700	534–538	19 655 ± 303	21 344 ± 205	22.00	1689	508	LGM		
MD01-2416	2317	88	12 690 ± 50	13 655 ± 55	13.66	965	105	B/A		Sarnthein et al. (2006)
MD01-2416	2317	96	12 555 ± 60	14 030 ± 70	13.50	1475	130	B/A		
MD01-2416	2317	115	13 205 ± 55	14 920 ± 70	14.27	1715	125	B/A		
MD01-2416	2317	136	13 090 ± 60	15 460 ± 80	14.04	2370	140	B/A		
MD01-2416	2317	163	13 795 ± 60	15 960 ± 100	15.50	2165	215	HS-1		
MD01-2416	2317	177	15 380 ± 70	17 850 ± 100	17.50	2480	170	HS-1		
ODP883	2385	51	12 715 ± 50	13 420 ± 90	13.68	705	140	B/A	Sarnthein et al. (2006)	
MD01-2420	2101	339.2–344.1	10 700 ± 55	12 100 ± 50	11.20	1400	105	YD	Okazaki et al. (2012)	
MD01-2420	2101	353.8–358.6	11 150 ± 55	12 400 ± 65	12.00	1250	120	YD		
MD01-2420	2101	370.7–375.6	11 717 ± 88	13 050 ± 60	12.70	1333	148	YD		
MD01-2420	2101	382.9–385.3	12 150 ± 50	13 450 ± 65	13.20	1300	115	B/A		
MD01-2420	2101	390.1–392.6	12 400 ± 45	13 750 ± 55	13.30	1350	100	B/A		
MD01-2420	2101	404.7–407.1	13 258 ± 141	14 600 ± 60	14.60	1342	201	B/A		
MD01-2420	2101	419.2–421.6	13 510 ± 113	14 750 ± 55	15.00	1240	168	HS-1		
MD01-2420	2101	431.3–433.7	13 900 ± 50	15 250 ± 60	15.50	1350	110	HS-1		
MD01-2420	2101	451.6–454.1	14 696 ± 70	15 850 ± 65	16.85	1154	135	HS-1		
MD01-2420	2101	489.2–494.2	16 450 ± 141	18 000 ± 75	18.75	1543	216			
MD01-2420	2101	504.1–506.6	17 020 ± 50	18 350 ± 70	19.45	1330	120	LGM		
Bering Sea (deep)										
SO201-2-77KL	2135	115	10 450 ± 40	11 650 ± 45	11.20	1200	85	Holocene		this study
SO201-2-77KL	2135	155	11 500 ± 50	13 000 ± 70	12.62	1200	85	YD		
SO201-2-77KL	2135	180	13 200 ± 45	14 450 ± 85	14.75	1250	130	B/A		

* Recalculated with a constant reservoir age correction of 700 yr for the Bering Sea and 900 yr for the NW-Pacific and Okhotsk Sea, respectively.

Pulses of enhanced North Pacific Intermediate Water ventilation

L. Max et al.

Title Page

Abstract

Introduction

Conclusions

References

Tables

Figures

⏪

⏩

◀

▶

Back

Close

Full Screen / Esc

Printer-friendly Version

Interactive Discussion



Pulses of enhanced North Pacific Intermediate Water ventilation

L. Max et al.

[Title Page](#)

[Abstract](#)

[Introduction](#)

[Conclusions](#)

[References](#)

[Tables](#)

[Figures](#)



[Back](#)

[Close](#)

[Full Screen / Esc](#)

[Printer-friendly Version](#)

[Interactive Discussion](#)

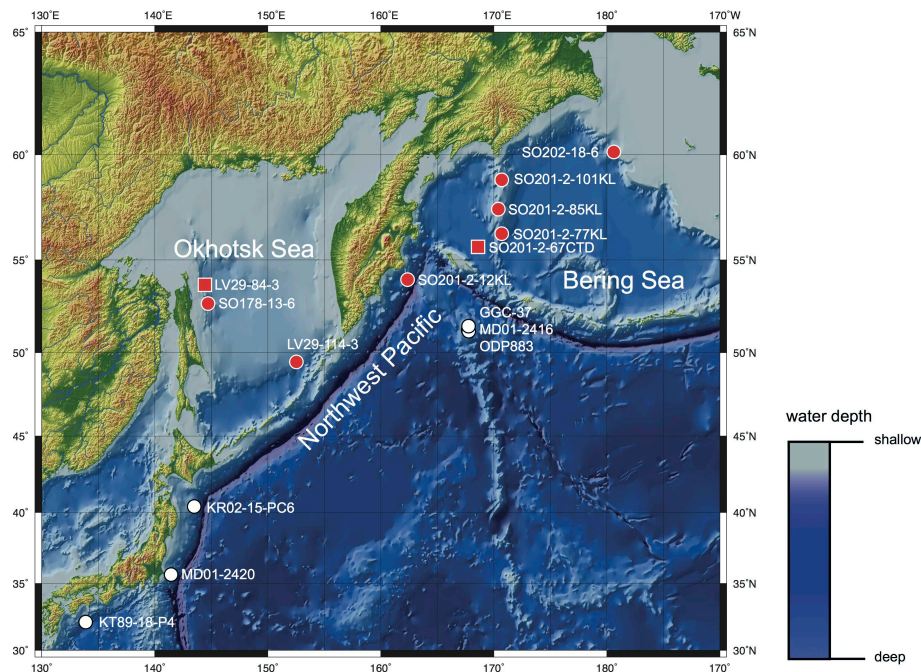
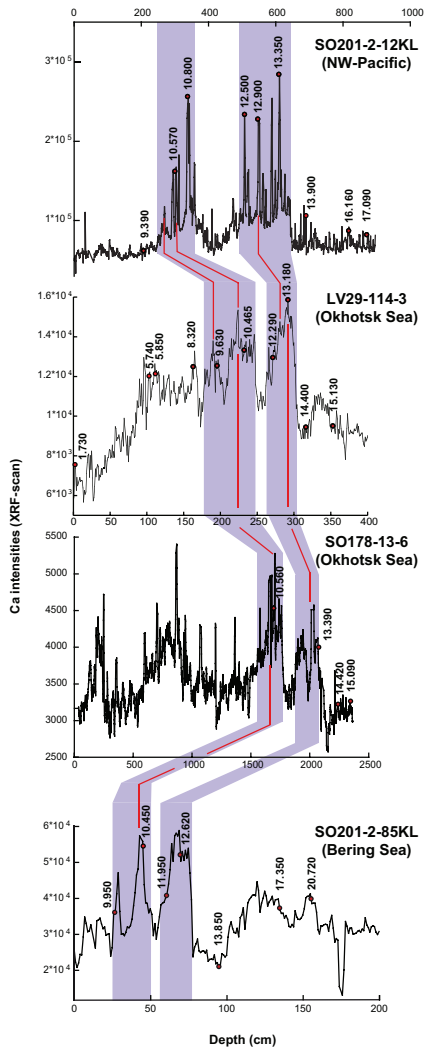


Fig. 1. Overview of the subarctic Northwest Pacific and its marginal seas (Okhotsk Sea and Bering Sea). Red spots indicate core locations and red squares mark hydrocast stations obtained in this study. White spots show published sediment cores from the Northwest Pacific realm considered in this study (please see Table 3 and references therein).



6248

CPD

9, 6221–6253, 2013

Pulses of enhanced North Pacific Intermediate Water ventilation

L. Max et al.

Title Page

Abstract

Introduction

Conclusions

References

Tables

Figures

⏪

⏩

◀

▶

Back

Close

Full Screen / Esc

Printer-friendly Version

Interactive Discussion



Pulses of enhanced North Pacific Intermediate Water ventilation

L. Max et al.

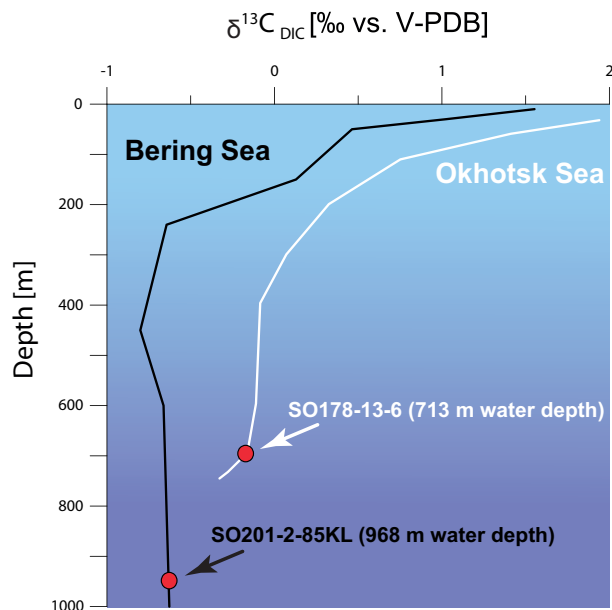


Fig. 3. Water column profiles of $\delta^{13}\text{C}_{\text{DIC}}$ in the Bering Sea (station SO201-2-67) and Okhotsk Sea (station LV29-84-3) given as $\delta^{13}\text{C}_{\text{DIC}}$ profile of the Bering Sea (in black) together with the respective depth-interval of SO201-2-85KL (red spot) and $\delta^{13}\text{C}_{\text{DIC}}$ profile for the Okhotsk Sea (in white) together with the corresponding depth-interval of SO178-13-6 (red spot).

[Title Page](#)[Abstract](#)[Introduction](#)[Conclusions](#)[References](#)[Tables](#)[Figures](#)[⏪](#)[⏩](#)[◀](#)[▶](#)[Back](#)[Close](#)[Full Screen / Esc](#)[Printer-friendly Version](#)[Interactive Discussion](#)

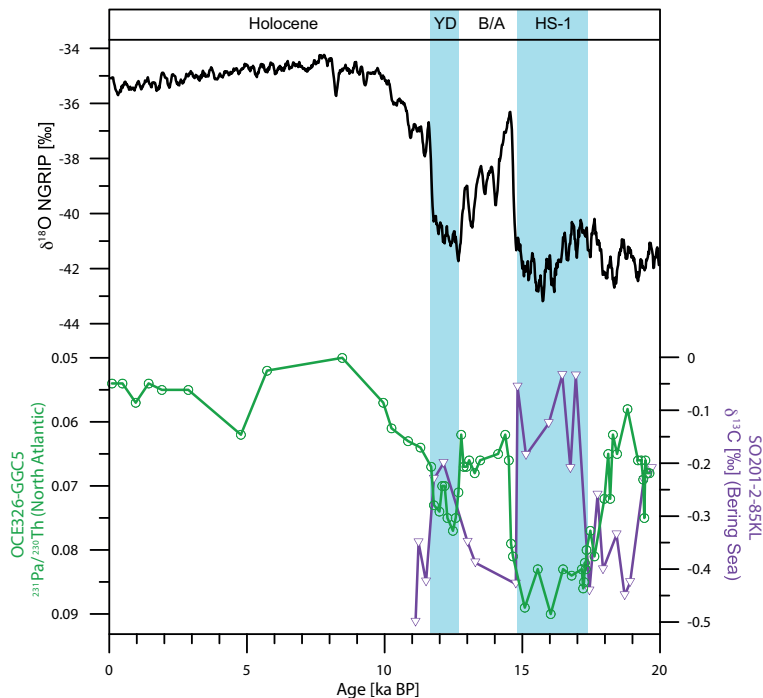


Fig. 4. Detailed comparison of deglacial circulation changes in the North Atlantic and Western Bering Sea during the past 20 kyr. Given are the Pa/Th ratio as proxy for the AMOC strength in the North Atlantic (in green) (McManus et al., 2004) compared to the Western Bering Sea intermediate-depth $\delta^{13}\text{C}$ record (in purple) as proxy for circulation changes in the Northwest Pacific. Blue shaded areas mark stadial HS-1 and the YD, respectively. For comparison, the NGRIP ice core record (in black) is given on top (Rasmussen et al., 2006).

Pulses of enhanced North Pacific Intermediate Water ventilation

L. Max et al.

[Title Page](#)

[Abstract](#) | [Introduction](#)

[Conclusions](#) | [References](#)

[Tables](#) | [Figures](#)

[◀](#) | [▶](#)

[◀](#) | [▶](#)

[Back](#) | [Close](#)

[Full Screen / Esc](#)

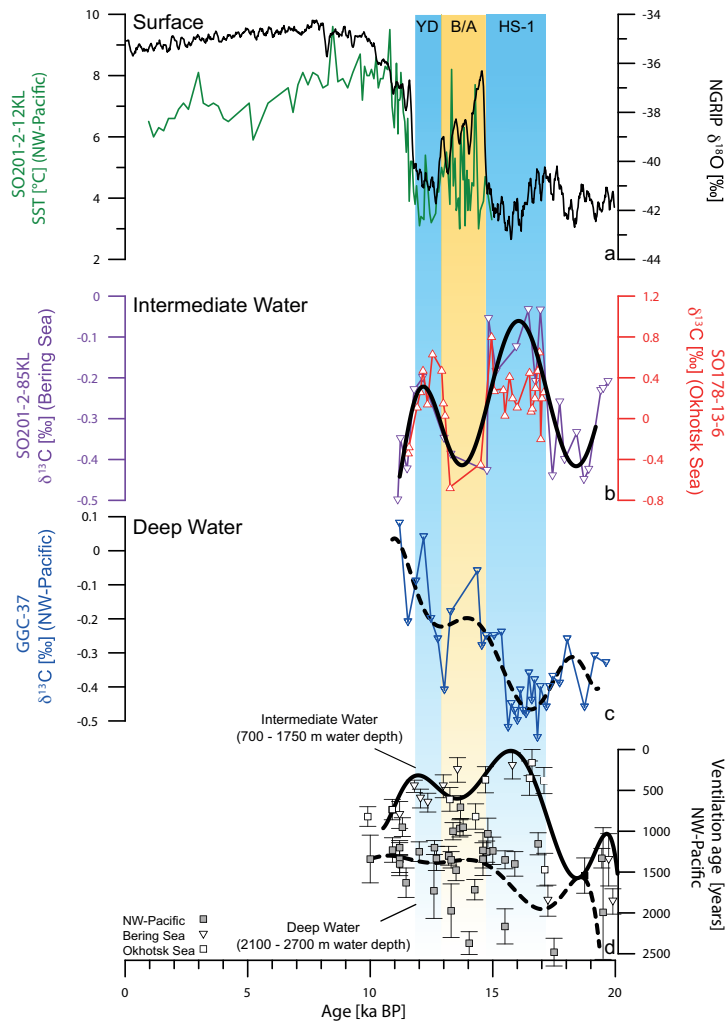
[Printer-friendly Version](#)

[Interactive Discussion](#)



Pulses of enhanced North Pacific Intermediate Water ventilation

L. Max et al.



[Title Page](#)

[Abstract](#) | [Introduction](#)

[Conclusions](#) | [References](#)

[Tables](#) | [Figures](#)

[◀](#) | [▶](#)

[◀](#) | [▶](#)

[Back](#) | [Close](#)

[Full Screen / Esc](#)

[Printer-friendly Version](#)

[Interactive Discussion](#)



Fig. 5. Sediment proxy records of changes in surface, intermediate and deep-water properties in the Northwest Pacific realm during the past 20 kyr. Blue and yellow shaded bars mark HS-1 and YD as well as the Bølling/Allerød interstadial, respectively. From top to bottom **(a)** alkenone-based sea surface temperature record of sediment record SO201-2-12KL (in green) from the Northwest Pacific (Max et al., 2012) for the last 15 kyr together with NGRIP oxygen isotope record in black (Rasmussen et al., 2006). **(b)** Benthic foraminiferal $\delta^{13}\text{C}$ -records (*C. lobatulus*) from the Okhotsk Sea (~ 700 m water depth; red curve) and Bering Sea (ca. 1000 m water depth; purple curve) together with smoothed spline interpolation of the records (thick black line) **(c)** benthic $\delta^{13}\text{C}$ -record from sediment record GGC-37 (Keigwin, 1998) from the deep Northwest Pacific (ca. 3300 m water depth, blue curve) and smoothed spline interpolation of the record (stippled black line) **(d)** Okhotsk Sea and Bering Sea Intermediate Water ventilation ages (700–1750 m water depth; open squares and triangles) compared to deep-water ventilation ages (2100–2700 m water depth; gray squares) of the Northwest Pacific (Duplessy et al., 1989; Murayama et al., 1992; Adkins and Boyle, 1997; Keigwin, 2002; Ahagon et al., 2003; Sarnthein et al., 2006; Minoshima et al., 2007; Sagawa and Ikehara, 2008; Okazaki et al., 2012) Calculated error bars are given for each estimated ventilation age. Smoothed spline interpolations for intermediate and deep-water ventilation ages are given by the thick black line (intermediate water) and thick stippled line (deep-water), respectively.

Pulses of enhanced North Pacific Intermediate Water ventilation

L. Max et al.

Title Page

Abstract

Introduction

Conclusions

References

Tables

Figures

⏪

⏩

◀

▶

Back

Close

Full Screen / Esc

Printer-friendly Version

Interactive Discussion